



HAL
open science

Robust molecular wind lidar with Quadri Mach-Zehnder interferometer and UV fiber laser for calibration/validation and future generation of Aeolus

Thibault Boulant, Matthieu Valla, Jean-François Mariscal, Nicolas Rouanet,
David Tomline Michel

► To cite this version:

Thibault Boulant, Matthieu Valla, Jean-François Mariscal, Nicolas Rouanet, David Tomline Michel. Robust molecular wind lidar with Quadri Mach-Zehnder interferometer and UV fiber laser for calibration/validation and future generation of Aeolus. SPIE Remote Sensing, 2023, SPIE, Sep 2023, Amsterdam, Netherlands. pp.127300M, 10.1117/12.2680187. hal-04395896

HAL Id: hal-04395896

<https://hal.science/hal-04395896>

Submitted on 15 Jan 2024

HAL is a multi-disciplinary open access archive for the deposit and dissemination of scientific research documents, whether they are published or not. The documents may come from teaching and research institutions in France or abroad, or from public or private research centers.

L'archive ouverte pluridisciplinaire **HAL**, est destinée au dépôt et à la diffusion de documents scientifiques de niveau recherche, publiés ou non, émanant des établissements d'enseignement et de recherche français ou étrangers, des laboratoires publics ou privés.

Robust molecular wind lidar with Quadri Mach-Zehnder interferometer and UV fiber laser for calibration/validation and future generation of Aeolus

Thibault Boulant^a, Matthieu Valla^a, Jean-François Mariscal^b, Nicolas Rouanet^b, and David Tomline Michel^a

^aONERA, 6 Chemin de la Vauve aux Granges, Palaiseau, France

^bLATMOS, 11 boulevard d'Alembert, Guyancourt, France

ABSTRACT

Wind speed measurement with on-board system has many applications in aeronautics (Gust Load alleviation, Haps, etc.) and space (Weather forecast). The molecular wind lidar is developed for those purposes as it sent laser pulses into the atmosphere to determine, with a spectral analyzer, the wind speed from the Doppler shift induced by the molecules of the atmosphere. In this paper we present the lidar architecture developed at ONERA, that uses a Quadri Mach-Zehnder (QMZ) as a spectral analyzer and a UV fiber laser, designed for gust load alleviation application. We discuss about the advantages of such architecture for wind measurement from space. Simulations of the performances have been performed in the case of Calibration/Validation (Cal/Val) of Aeolus, showing standard deviation on wind speed measurement less than 2 m/s up to 17 km of altitude for the optimized hybrid fiber laser of 10 W laser average power and a pulse repetition frequency (PRF) of 5 kHz. Simulations that evaluates the performances for Aeolus measurement with minor changes in the lidar architecture have been computed, with results showing that requirements are fulfilled up to 22.5 km of altitude with the optimized hybrid fiber laser of 10 W and 3 kHz PRF.

Keywords: molecular wind lidar, Quadri Mach-Zehnder, fiber laser

1. INTRODUCTION

The wind measurement with embedded atmospheric lidar have many applications such as gust load alleviation,¹⁻⁴ navigation aid for aircraft navigation⁵ or high-altitude platform system,⁶ weather forecasting improvement using wind measurements from spaceborne lidar.⁷ The latter was realized during the ADM-Aeolus mission, launched in 2018, providing the first global wind profiles from space across the entire troposphere and lower stratosphere which led to a significant improvement in the weather forecast score.⁸ To achieve the 2 m/s velocity measurement precision required for Aeolus up to 16 km,⁹ the mission places high demands on instrument characteristics such as alignment stability, compactness, fringe contrast, sensitivity to the spectral shift, resistance to vibrations and thermal gradient. In order to verify the overall performance, comparative measurements should be performed, especially with other wind lidar. In this respect, the use of onboard lidar makes it possible to follow the measurements made by the satellite and to bring the lidar to high altitude in order to improve the precision of the measurement. On the other hand, optimizing the technologies used to design Aeolus could lead to better performance, in particular better precision, greater longevity or lower weight, which would lead to a reduction in the overall cost of the mission and/or further improve the weather forecast score. For these two reasons, the exploration of new lidar technologies is very important for the mission and the continuation of Aeolus.

Wind lidars are instruments that measure wind speed remotely. A laser emits pulses into the atmosphere and the velocity is deduced from the Doppler frequency shift induced by the speed of molecules and particles

Further information : The project 101101974 – UP Wing is supported by the Clean Aviation Joint Undertaking and its members.

Funded by the European Union. Views and opinions expressed are however those of the author(s) only and do not necessarily reflect those of the European Union or Clean Aviation Joint Undertaking. Neither the European Union nor the granting authority can be held responsible for them.

on backscattered light using a spectrum analyzer. For wind measurements at all altitudes, molecular lidar are used as molecules are present in the entire atmosphere. For such measurement, UV laser is preferred to improve the backscattered light intensity ($\propto 1/\lambda^4$). To determine the spectral shift of the backscattered light, an interferometer is typically used¹⁰⁻¹³ to obtain an interference figure that depends on the optical frequency of the input light. By comparing the interference figure obtained for the backscattered light with the one obtained for the laser, the Doppler frequency shift is measured, and then the wind velocity.

Several molecular wind lidar architectures have been developed and used for Aeolus calibration/validation and for Aeolus measurements. A first set-up consists in using a double-edge Fabry-Perot interferometer as a spectral analyzer. This set-up is used for ground based lidars of the Observatoire de Haute Provence and Observatoire de Physique de l'Atmosphère de la Réunion observations sites,¹⁴ the lidar embedded in Aeolus named ALADIN and the ALADIN Airborne Demonstrator (A2D).¹⁵ This spectral analyzer consists of two coupled Fabry-Perot interferometers, placed on either side of the Rayleigh spectrum: when the spectrum is shifted in frequency the light ratio between the two channel varies. The main disadvantage of this technique comes from the dependence on the shape of the spectrum, which depends on the atmospheric temperature and pressure,¹⁶ and also depends on the amount of scattering from particles in the collected signal.¹⁷ Indeed, a change in the shape of the spectrum induces a modification of the ratio of light passing through each filter. For ALADIN and A2D, a Mie channel using a Fizeau interferometer has been added. This channel is used to retrieve the backscattering ratio and correct the bias induced by Mie scattering on the Rayleigh channel measurement. A second type of spectral analyzer is the Michelson interferometer, that first has been studied at ONERA¹⁸ and developed in a monolithic design for on-board application by the DLR.¹³ This interferometer is set to give linear interference fringes on a multi-pixel detector of the incident light, where the position of the fringes depends on the optical frequency. This technique has several disadvantages including the difficulty of accessing the second output of the interferometer which goes in the backward direction with a very small angle (almost superposed to the input beam). Not analyzing the second output reduce the total intensity of the analyzed signal by a factor of 2 which lead to a decrease of the signal-to-noise ratio (SNR) by a factor of $\sqrt{2}$. Also the use of the imaging detector often requires adapting the circular pupil of the beam to the square shape of the detector and some signal is lost due to the spacing between the pixels. All these effects reduce the SNR resulting in an increase of the error on the estimation of the wind speed. The third type of spectral analyzer is the QMZ interferometer^{19,20} that have been developed for airborne wind measurement and have also been tested for Cal/Val campaigns of Aeolus. The cat-eye design allows to field widened the interferometer which reduces sensitivity to beam divergence. However, the number of optics increase the alignment complexity and the risk of having optics disrupt by vibrations in flight. All those lidar use 1 μm solid states laser where a laser diode is injected in the optical cavity to maintain a narrow spectrum and stabilize the wavelength value. However, this requires to keep the cavity length adapted to the wavelength of the laser diode which requires to control the cavity length within less than 1 μm with a feedback loop. In addition such design is expensive, heavy and difficult to use in space because they cannot operate in vacuum environment. For Aeolus a continuous injection of oxygen is required to avoid damages optical surfaces which further increase the difficulty to operate such laser in space.

In this paper, we present a molecular wind lidar developed at ONERA that use a monolithic QMZ spectral analyzer and a UV fiber for airborne wind speed measurement. The combination of these two bricks allows to increase robustness to vibrations, to have a strong signal at the output of the detector and to have a large angular acceptance of the spectral analyzer. This lidar is currently developed to measure turbulence in front of an aircraft. We investigate with simulations the possibility to use this lidar for Cal/Val applications with minor changes. Then, we study with simulations how it should be modified to be used for the future Aeolus mission and the advantages of such architecture.

2. UV LIDAR ARCHITECTURE

In the frame of the clean aviation project we develop a UV lidar for future aircraft with larger wings designed to reduce aircraft consumption. The lidar will be used to measure turbulences in front of the aircraft to modify the wing shape to reduce the load of the air on the wings using actuators that modify the aircraft aerodynamic profile according to the direction and strength of the wind. Indeed, larger wings are more sensitive to turbulence and requires such technique (called gust load alleviation). The lidar is configured to measure the wind between 100 m

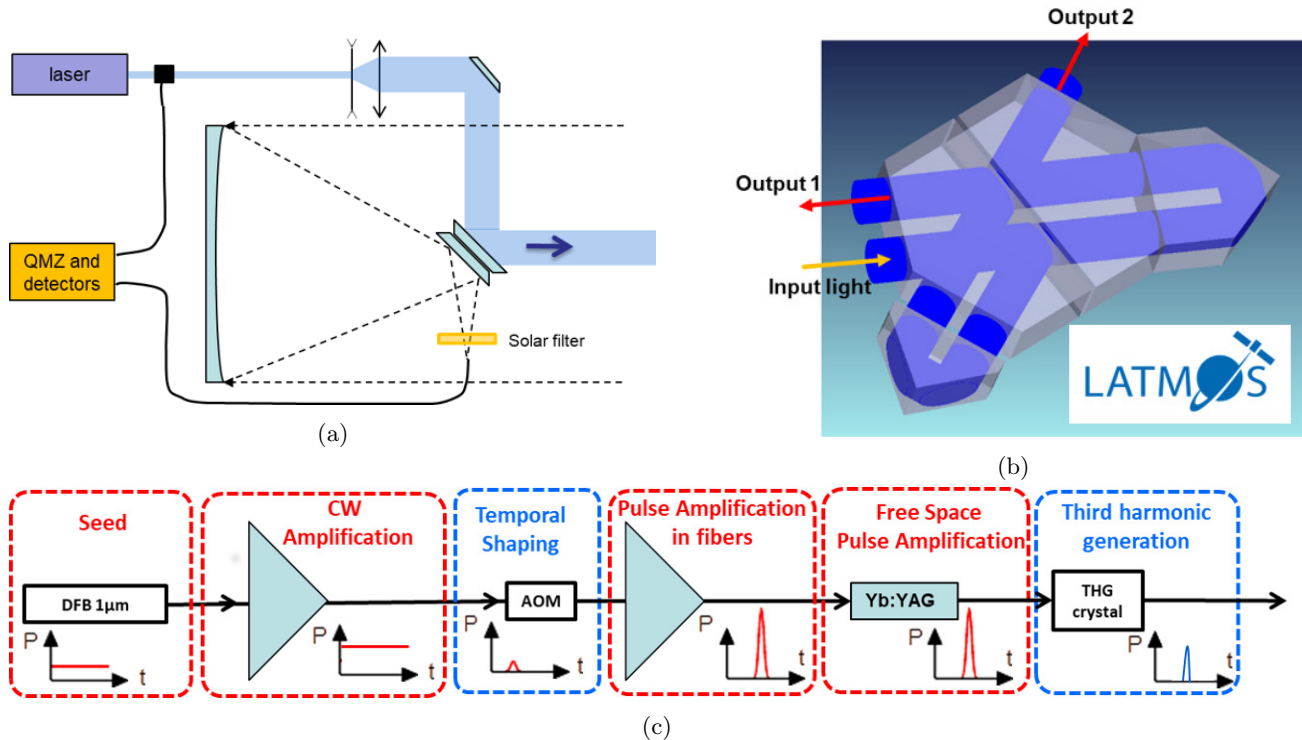


Figure 1: (a) schematic of the UV molecular wind lidar (b) The monolithic Quadri Mach-Zehnder (c) schematic of the hybrid fiber laser

and 300 m ahead of the aircraft, with a spatial resolution of 10 m, a precision of 1 m/s with an integration of 100 ms. The schematic of the UV molecular wind lidar developed at ONERA is presented in Fig. 1a. The system is separated in three main part: the laser system, the emission/reception telescope and the QMZ interferometer. The laser system emits about 10 ns UV pulses that pass through a beam expander to have a beam diameter of about 4 cm and are sent out into the atmosphere. Backscattered light from molecules and particles is collected by a 6 inch Newton telescope with a geometrical aperture of 4 which focuses the light into an optical fiber of 400 μm -core diameter. An interference filter of 1 nm bandwidth makes it possible to reject the part of the broad spectrum coming from the scene captured by the telescope. The collected signal is sent to the QMZ and followed temporally by a sample of the laser taken just after the laser output. The QMZ interferometer splits the incident beam into two beams of equal intensity using a 50/50 beam splitter. The two beams pass through two arms with different optical paths and are recombined on a second beam splitter. A quarter-wave plate on an arm increases the optical path of a vertical polarization state relative to the horizontal polarization state. The two polarization states are separated at the two outputs with polarization separator cubes and four interference states out of phase by $\pi/2$ are obtained (i.e. separated by $0, \pi/2, \pi, 3\pi/2$). The intensity of the four interferences is a function of the optical frequency of the incident light. The difference in intensity between the collected signal and the laser gives the frequency offset and therefore the wind speed.²¹

In order to obtain a robust design insensitive to misalignment caused by flight vibrations, a monolithic QMZ interferometer [Fig.1b] is currently under development in collaboration with the LATMOS Laboratory. The interferometer consists of four prisms held together by molecular adhesion or glue to form a monolithic interferometer. Some faces are coated to achieve equal intensity separation of light and to maximize the overall transmission of the interferometer. A mechanical structure is also developed to minimize thermal gradient and to further increase robustness to vibration in typical aircraft environment.

To further improves robustness of the system, a fiber laser is currently studied and developed according to the architecture shown in Fig. 1c. A distributed feedback (DFB) laser diode emits 1 μm continuous beam, that is amplified by a pumped doped fiber. Pulses are generated with an acousto optic modulator and are amplified

by another pumped doped fiber. The third harmonic generation crystal is used to have a 0,34 μm pulse beam. A free space amplification crystal may be added to the architecture to increase the energy of the laser (hybrid fiber laser). We can note that this instruments had additional advantages including efficiency, cheaper components and the ability to shape temporally the pulses to optimize them for the lidar measurements. We can also notice that a free-space amplifying crystal is quite robust to misalignment.²²

For the current study three different laser are planned : a commercial solid states laser, the MerionC from Quantel with energy per pulse of 22.5 mJ and a PRF of 400 Hz, a fiber laser of 40 kHz and 250 μJ , and a hybrid fiber laser with free-space amplification stage of 40 kHz and 750 μJ .

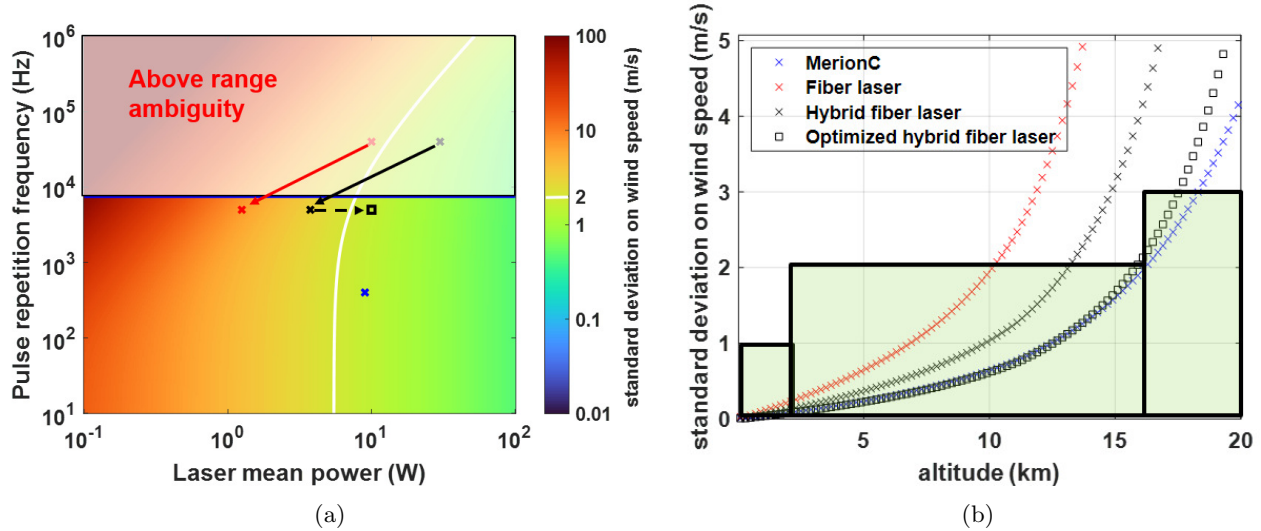


Figure 2: (a) wind speed standard deviation as a function of the laser mean power and the pulse repetition frequency at 15 km altitude. Blue cross: MerionC; red cross: fiber laser; black cross: hybrid fiber laser; black square: optimized hybrid fiber laser of 10 W. The blue line represent the PRF limit that correspond to the range ambiguity of 20 km. The white line represent 2 m/s limit (b) wind speed standard deviation as function of altitude for the three laser. Green rectangles indicate the Aeolus requirements according to the Mission Requirements Document⁹

3. CALIBRATION/VALIDATION APPLICATION

In this part, we evaluate the performance of the UV lidar for Calibration/Validation of Aeolus with minimum changes in the architecture. The lidar performances are evaluated using simulations. To evaluate the performances, we estimate the precision of the wind speed measurement. The simulator include three parts:

- the first part calculates the molecular backscatter coefficient and atmospheric transmission along the line-of-sight of the lidar. In this purpose, the molecular backscatter and extinction coefficients are evaluated at each altitude using the temperature and pressure given by the 1976 Standard Atmosphere Model²³

- the second part determines the flow of photons collected as a function of distance (deduce from the time accounting for the speed of light). At each distance, the lidar signal is average over a spacial distance, called range gate, to improve the SNR but reduce the spatial resolution.

- the last part firstly computes the contribution of each noise sources on the SNR. The total noise includes the shot noise of the backscattered signal, the shot noise of the background signal, the Speckle noise and the detection noise, that include dark noise from the detector and electronic noise. The detection noise is negligible because of the use of Photo-multiplier tube that amplified the collected signal. The Speckle noise from the signal is also negligible because the beam size and the coherence length (compared to the range gate) lead to a strong averaging of the Speckles. Then the SNR is calculated at each range by dividing the number of photons per the quadratic summation of the two shot noises. To evaluate the precision of the retrieved wind speed, we use the

formula that gives the standard deviation presented in the paper of Bruneau and Pelon part 2.B.²¹ We can note that this formula is calculated for a specific signal processing method. However, we did comparison with the Cramer-Rao boundary and excellent agreement were obtained.

To evaluate the performance of the lidar for Cal/Val application, we have performed simulations using the same lidar optics as presented previously. We consider that the lidar is located on the ground and its line-of-sight goes toward the zenith, the range gate is equal to 200 m and the measurement is integrated over 2 s. The background radiation power was taken equal to $0.001W/m^2/str/nm$ which is similar to the one taken in ref.⁷ The PRF of the laser had to be decreased to avoid pulse overlapping between the one reflected at the end and the following one reflected at the beginning of the atmosphere (called range ambiguity). As the measurement have to be made up to 20 km, the corresponding PRF limit is $c/(2 * d_{max})=5000$ Hz where c is the light celerity and $d_{max}=20$ km. The PRF of the two fiber laser, chosen for on-board application, are too high and so they are not adapted to the study. However, it is possible to decrease the PRF down to 5 kHz using pulse picking that consist of taking one pulse over a certain number of pulses, while maintaining the same energy per pulse. The final mean power would be around 1.25 W for the fiber laser and 3.75 W for the hybrid fiber laser.

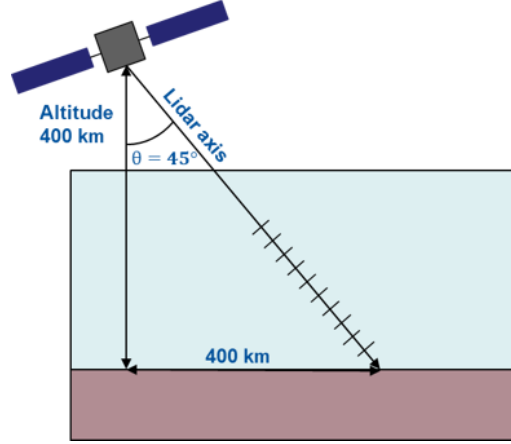
Simulations of the evolution of the standard deviation as a function of the PRF and laser average power have been performed for an altitude of 15 km and the result is shown in Fig. 2a. As the precision decrease with altitude, fulfilling the requirement of Aeolus is equivalent to have a lidar that have a standard deviation below 2 m/s at this altitude. This simulation evaluate the optimization of the laser for wind speed measurement. The parameter of the three laser used for the project of the ONERA UV wind lidar have been placed on the figure. We also represent the two fiber laser with lower PRF. The result shows that only the MerionC fulfill the requirements at 15 km. However, we decrease here the PRF of the fiber laser considering that we only use pulse picking. However, previous experiment suggest that it is also possible to decrease the laser PRF at constant average power down to about 15 kHz by reducing the PRF of the initial laser diode but keeping the same diode pump power. If we consider that pulse picking is used in a second time to reduce the PRF down to 5 kHz, we obtain an average power of 10 W for the hybrid fiber laser (square on the figure) and the laser fulfills Aeolus requirements at 15 km. Another possibility is to increase the integration time to increase the SNR.

To verify if the requirements of Aeolus are met, simulations were performed to determine the wind speed standard deviation as a function of altitude for the three laser [fig.2b]. The results show that the MerionC meets the requirements up to 17.5 km, the fiber laser up to 10 km and the hybrid fiber laser up to 12.5 km. If we assume a 10 W average power hybrid fiber laser (optimized on the figure), the requirements are fulfilled up to 17 km of altitude.

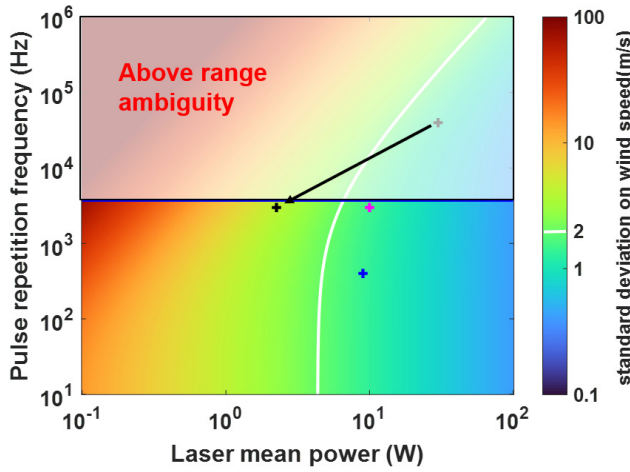
4. AEOLUS TYPE MEASUREMENTS ASSESS BY SIMULATION

In this part, we evaluate the performance of the UV lidar for Aeolus wind measurement with minimum changes in the architecture. We assume the initial Aeolus requirements as mentioned in the Aeolus Mission Requirements Document⁹ (that differ from the last Aeolus design). Fig. 3a presents the geometry of Aeolus measurement. The satellite is located at 400 km of altitude and the angle of the line-of-sight of the lidar is 45° from nadir. The measurement has a range gate equal to 707 m to give a vertical resolution of 500 m. The satellite speed ($7.2km.s^{-1}$) and the integration time of 7 s give a horizontal resolution of 50 km. Simulation have been performed with the same parameters as the one presented in the paper of Bruneau and Pelon:⁷ the telescope is a 1.5 m mirror, with a 0.1 mrad field of view, the interferential filter bandwidth is 0.1 nm. For the laser parameter, we adopted the same strategy as for the previous Cal/val simulation, except that the range ambiguity of 40 km is assumed and we only consider the hybrid fiber laser. The PRF of the hybrid fiber laser of 3 kHz is chosen to be below the PRF limit imposed by the range ambiguity. We only consider pulse picking that give an average power of 2.25 W.

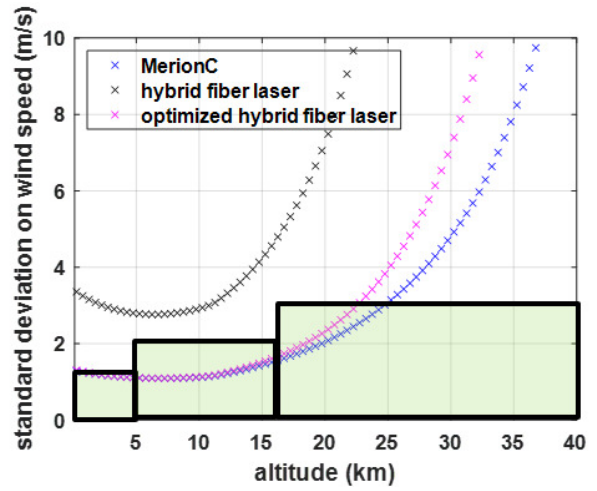
Simulation of the evolution of standard deviation as a function of PRF and laser average power have been performed for an altitude of 15 km and the result is shown in Fig. 3b. The results show that the MerionC fulfill the requirements at 15 km but not the hybrid fiber laser. To meet the requirements with the hybrid fiber laser, it is possible to decrease the laser PRF at constant average power down to about 15 kHz and then do pulse picking at 3 kHz to reach average power of 6 W . Moreover, free space amplifier could be added to reach an average power of 10 W (magenta cross) to fulfill the Aeolus requirements at 15 km.



(a)



(b)



(c)

Figure 3: (a) Schematic of the Aeolus measurement with the new parameters⁷ (b) Standard deviation on wind speed measurement with Aeolus at 15 km altitude. The blue line represent the PRF limit that correspond to the range ambiguity of 20 km, The white line represent 2 m/s limit. Blue cross: MerionC; black cross: hybrid fiber laser; magenta cross: optimized hybrid fiber laser. (c) Standard deviation on wind speed as a function of altitude. Green rectangles indicate the Aeolus requirements according to the Mission Requirements Document⁹

To evaluate the performances of the two laser, standard deviation as a function of the altitude have been computed and the results are presented in Fig. 3c. The results show that the MerionC fulfill the requirements up to 25 km and the hybrid fiber laser gives a standard deviation above the requirements at all altitude. Then it is necessary to use the optimized hybrid fiber laser of 10 W that reach the requirements up to 22.5 km of altitude. Note that it is also possible to increase the integration time by a factor 2 as it is the case for Aeolus to improve the precision by a factor $\sqrt{2}$.

5. CONCLUSION

A robust lidar architecture comprising a monolithic QMZ interferometer and a hybrid fiber laser was presented. Simulations were performed to evaluate the performances of such architecture for Cal/Val of Aeolus and for future Aeolus generations. For Cal/Val, simulations show that Aeolus requirements of 2 m/s are fulfilled at all altitude below 16 km with the MerionC and the hybrid fiber laser of 5 kHz and 10 W average power. For future Aeolus generation, the requirements are met up to 25 km of altitude for the MerionC and up to 22.5 km of altitude for the hybrid fiber laser of 10 W and 3 kHz.

ACKNOWLEDGMENTS

Our thanks to Pierre Pichon, Jonathan Pouillaude and Laurent Lombard for the valuable discussion on the fiber laser.

REFERENCES

- [1] Soreide, D. C., Bogue, R. K., Ehernberger, L., and Bagley, H. R., “Coherent lidar turbulence for gust load alleviation,” in [*Optical Instruments for Weather Forecasting*], **2832**, 61–75, SPIE (1996).
- [2] Fournier, H., Massioni, P., Tu Pham, M., Bako, L., Vernay, R., and Colombo, M., “Robust gust load alleviation of flexible aircraft equipped with lidar,” *Journal of Guidance, Control, and Dynamics* **45**(1), 58–72 (2022).
- [3] Cavaliere, D., Fezans, N., Kiehn, D., Quero, D., and Vrancken, P., “Gust load control design challenge including lidar wind measurements and based on the common research model,” in [*AIAA Scitech 2022 Forum*], 1934 (2022).
- [4] de Souza, A. d. R., Vuillemin, P., Quero, D., and Poussot-Vassal, C., “Observer-based gust load alleviation via reduced-order models,” *IFAC-PapersOnLine* **55**(25), 25–30 (2022).
- [5] Augere, B., Besson, B., Fleury, D., Goular, D., Planchat, C., and Valla, M., “1.5 μm lidar anemometer for true air speed, angle of sideslip, and angle of attack measurements on-board piaggio p180 aircraft,” *Measurement Science and Technology* **27**(5), 054002 (2016).
- [6] Strganac, T., “Wind study for high altitude platform design,” in [*3rd Lighter-Than-Air Systems Technology Conference*], 1607 (1979).
- [7] Bruneau, D. and Pelon, J., “A new lidar design for operational atmospheric wind and cloud/aerosol survey from space,” *Atmospheric Measurement Techniques* **14**(6), 4375–4402 (2021).
- [8] Rennie, M., Stoffelen, A., Khaykin, S., Osprey, S., Wright, C., Banyard, T., Straume, A. G., Reitebuch, O., Krisch, I., Parrinello, T., et al., “Demonstrated aeolus benefits in atmospheric sciences,” in [*2021 IEEE International Geoscience and Remote Sensing Symposium IGARSS*], 763–766, IEEE (2021).
- [9] ADM-Aeolus, Mission Requirements Document, ESA, AE-RP-ESA-SY-001 EOPSM/2047, Issue 2, 57 pp.,2016.
- [10] Flesia, C. and Korb, C. L., “Theory of the double-edge molecular technique for doppler lidar wind measurement,” *Applied Optics* **38**(3), 432–440 (1999).
- [11] Bruneau, D., “Mach-zehnder interferometer as a spectral analyzer for molecular doppler wind lidar,” *Applied Optics* **40**(3), 391–399 (2001).
- [12] Bruneau, D., “Fringe-imaging mach-zehnder interferometer as a spectral analyzer for molecular doppler wind lidar,” *Applied optics* **41**(3), 503–510 (2002).
- [13] Herbst, J. and Vrancken, P., “Design of a monolithic michelson interferometer for fringe imaging in a near-field, uv, direct-detection doppler wind lidar,” *Applied Optics* **55**(25), 6910–6929 (2016).
- [14] Ratynski, M., Khaykin, S., Hauchecorne, A., Wing, R., Cammas, J.-P., Hello, Y., and Keckhut, P., “Validation of aeolus wind profiles using ground-based lidar and radiosonde observations at réunion island and the observatoire de haute-provence,” *Atmospheric Measurement Techniques* **16**(4), 997–1016 (2023).
- [15] Lux, O., Lemmerz, C., Weiler, F., Marksteiner, U., Witschas, B., Rahm, S., Geiß, A., and Reitebuch, O., “Intercomparison of wind observations from the european space agency’s aeolus satellite mission and the aladin airborne demonstrator,” *Atmospheric Measurement Techniques* **13**(4), 2075–2097 (2020).
- [16] Zhai, X., Marksteiner, U., Weiler, F., Lemmerz, C., Lux, O., Witschas, B., and Reitebuch, O., “Rayleigh wind retrieval for the aladin airborne demonstrator of the aeolus mission using simulated response calibration,” *Atmospheric Measurement Techniques* **13**(2), 445–465 (2020).
- [17] Witschas, B., Lemmerz, C., Geiß, A., Lux, O., Marksteiner, U., Rahm, S., Reitebuch, O., and Weiler, F., “First validation of aeolus wind observations by airborne doppler wind lidar measurements,” *Atmospheric Measurement Techniques* **13**(5), 2381–2396 (2020).
- [18] Cezard, N., *Etude de faisabilité d’un lidar Rayleigh-Mie pour des mesures à courte portée de la vitesse de l’air, de sa température et de sa densité*, PhD thesis, Palaiseau, Ecole polytechnique (2008).

- [19] Tucker, S. C., “Owl: A high-heritage us doppler wind lidar for next-generation space-based wind and aerosol observations,” (2018).
- [20] Tucker, S., Applegate, J., Walters, B., and Weimer, C., “Quadrature mach zehnder interferometers for lidar remote sensing of winds and aerosols in the planetary boundary layer through the lower stratosphere,” in [*Propagation Through and Characterization of Atmospheric and Oceanic Phenomena*], JTU5F-4, Optica Publishing Group (2020).
- [21] Bruneau, D. and Pelon, J., “Simultaneous measurements of particle backscattering and extinction coefficients and wind velocity by lidar with a mach–zehnder interferometer: principle of operation and performance assessment,” *Applied Optics* **42**(6), 1101–1114 (2003).
- [22] Pouillaude, J., Pichon, P., Delen, X., Georges, P., and Lombard, L., “Amplification d’impulsions monofrequences et nanosecondes dans des fibres dopées yb courtes: 1030 nm ou 1064 nm ?,” J. Atmos. Ocean. Technol., Journée nationale d’optique guidée, 2023.
- [23] Oceanic, N. and Administration, A., “Us standard atmosphere, 1976,” *Technical Report* (1976).